# Preparation and Comparison of Two Electrodes for Supercapacitors: Pani/CNT/Ni and Pani/Alizarin-Treated Nickel

**Ozcan Koysuren,[1,2] Chunsheng Du,[2] Ning Pan,[2] Goknur Bayram[1]**

[1]*Department of Chemical Engineering, Middle East Technical University, Ankara 06531, Turkey*
[2]*Department of Biological and Agricultural Engineering, Division of Textiles, University of California, Davis 95616, California*

Received 2 September 2008; accepted 6 December 2008
DOI 10.1002/app.29924
Published online 2 April 2009 in Wiley InterScience (www.interscience.wiley.com).

**ABSTRACT:** Polyaniline in emeraldine form was synthesized in the presence of multiwalled carbon nanotubes (CNTs), and the electrochemical capacitance performance of thus formed composite as electrode material has been studied. The polyaniline/carbon nanotubes (Pani/CNT) composite is found to result in a higher specific capacitance than that of either composite constituent, attributable to the double-layer capacitance behavior of the nanotubes in the Pani/CNT system. However, once assembled into a two-electrode cell, lower than expected specific capacitance values from 1 to 20 F/g were obtained, and such reduction is most likely caused by the contact resistance between the Pani/CNT electrodes and the nickel (Ni) current collectors. To improve the situation, a chemical treatment was applied to the nickel foil, and the Pani solution is then deposited on the surface of the foil to form a coated structure (Pani/Ni). The thickness and weight of the Pani films can be controlled by adjusting the concentration of the Pani solution. The specific capacitance of the cell with electrodes made of the new Pani/Ni composite was found to reach as high as 35.5 F/g. © 2009 Wiley Periodicals, Inc. J Appl Polym Sci 113: 1070–1081, 2009

**Key words:** electrochemical supercapacitor; polymer-coated carbon nanotubes; nickel surface treatment; electrodes with polyaniline coating

## INTRODUCTION

There has been great interest in the investigation of electrode materials for electrochemical supercapacitors, which provide higher power density than conventional batteries and higher energy density than the dielectric capacitors.[1] Huge potential areas for such electrochemical supercapacitors include any applications where intense pulse power supply and fast charge and discharge cycles are required, typically in military weapon systems, in computer memory backup systems, and as power-storage devices operating in parallel with the battery in an electric vehicle.[1] Different from conventional batteries, electrochemical supercapacitors have almost unlimited cycling ability because no chemical and phase changes are involved in their charging and discharging processes.[2] Electrochemical supercapacitors store energy by utilizing double-layer and pseudocapacitance processes.[3] Therefore, to achieve high performance for such capacitors, the electrode material should have a high surface area, a high double-layer capacitance, and pseudocapacitance.[3]

The multiwalled carbon nanotubes (CNTs) have been considered as ideal electrode material for electrochemical supercapacitors, owing to the high specific surface area, low electrical resistivity, and nanoporous morphology to provide good electrolyte accessibility into the inner surface area of the electrode material, resulting in high specific capacitance (F/g).[4–12] CNTs have double-layer capacitance characteristics in which capacitance generation and charge–discharge processes are mainly electrostatic, that is, involving only the separation of ions and electrons.[13] Electrochemical capacitors with electrodes fabricated by depositing CNTs from their suspension showed a specific capacitance of 20 F/g,[11] and Du and Pan[12] obtained a specific capacitance of 21 F/g with CNTs-based electrodes readily prepared by electrophoretic deposition.

In addition, conducting polymers have also been regarded as alternative electrode material for electrochemical supercapacitors, owing to their pseudocapacitive behaviors.[2] These materials can be switched between the conducting and the insulating states by pseudocapacitive redox reactions known as the doping processes,[1] leading to electron transfer across the electrode and electrolyte interface. As capacitance is defined as the change in the amount of charge with

*Correspondence to:* N. Pan (npan@ucdavis.edu).
Contract grant sponsor: Faculty Development Programme of METU; contract grant number: BAP-08-11-DPT2002K120510.

a change in potential, redox reactions, which induce pseudocapacitance, hence contribute to the double-layer capacitance by changing the number of mobile charges.[13] Besides, doping processes are reversible, which makes the conducting polymers another group of attractive electrode materials. Polyacetylenes, polyanilines, and polyheterocycles, including both polypyroles and polythiophenes, are known to be among the most common conducting polymers. However, due to environmental instability of polyacetylene, most studies are focused on polyanilines and polyheterocycles.[1] Among these conducting polymers, much effort has been devoted to the use of polyaniline (Pani) as electrode material in electrochemical supercapacitors,[14–21] to replace the conventional electrode material for substantial improvements in performance, design, and cost. Zou et al.[17] and Girija and Sangaranarayanan[18] obtained specific capacitance values of 149 and 101 F/g, respectively, for a two-electrode cell by depositing Pani on a current collector.

Recently, several attempts have been made to combine the double-layer capacitance behavior of CNTs with pseudocapacitive characteristics of Pani.[22–24] CNTs with high specific surface area and low resistivity turn the coated Pani film into a nanoporous system of three-dimensional morphology.[22,23] Pani film with an enormous effective surface area of CNTs results in enhanced double-layer capacitance and pseudocapacitance because ions can diffuse and migrate easily in the active layer of the film.[15] Hence, Pani-coated nanotube electrodes have exhibited even higher specific capacitance than pure Pani and pure nanotube electrodes.[22,24] For instance, the specific capacitance value of Pani/CNT composite containing 80 wt % Pani was around 90 F/g for a two-electrode cell,[23] and Gupta and Miura[24] obtained a specific capacitance value of 115 F/g for a two-electrode cell by electrochemical deposition of Pani onto CNT.

In the present study, the electrochemical capacitance performance of Pani-coated CNTs over a wide range of compositions is investigated. The coating of Pani onto CNTs was carried out by chemical oxidative polymerization in the presence of CNTs. One existing problem with electrodes made of Pani/CNT composites is the poor adhesion between the electrode material and the current collector, resulting in high contact resistance and low capacitance. A chemical treatment was thus applied to the current collectors before the Pani films were coated.

## MATERIALS AND METHODS

### Growth of carbon nanotubes

The multiwalled CNTs used for electrochemical capacitor application were prepared by chemical vapor deposition method in our lab, and the resulted CNTs were cleaned and treated according to the procedures given in the literature.[11]

### Synthesis of polyaniline and polyaniline/carbon nanotube composites

The composite of doped Pani with multiwalled CNTs was prepared via an *in situ* polymerization method. Aniline hydrochloride (Alfa Aesar, Ward Hill, MA) was dissolved in ethanol to provide 0.04*M* aniline solution and ammonium peroxydisulfate (Alfa Aesar) dissolved in distilled water to yield 0.05*M* oxidant solution. Various weight ratios of nanotubes were added in the 0.04*M* aniline solution and stirred for 1 h.[25,26] As multiwalled CNTs are good electron acceptors and aniline is known as fine electron donors, aniline monomers and CNTs thus form a charge-transfer complex, resulting in adhesion of the aniline monomers onto the nanotubes.[27] The oxidant solution was then added into the aniline/CNTs mixture to start the polymerization. Aniline monomers adsorbed onto the nanotubes lead to the subsequent formation of Pani in emeraldine salt form. Following 24 h of stirring, the Pani-coated nanotubes were filtered under vacuum and rinsed with 0.2*M* hydrochloric acid solution to both remove residual monomers and generate more uniform doping of Pani with chloride ions. Next, the Pani/CNT composite particles were rinsed with acetone to clean up the oligomers to prevent any aggregation, before being dried at 60°C for 24 h.[25,26] Such composites, containing 10, 20, 40, 60, and 80 wt % Pani, were thus prepared (Table I). In addition to Pani/CNT composites, pure Pani was also synthesized in the emeraldine salt form and a portion of synthesized Pani salt was converted to the emeraldine base form by using 1*M* ammonium hydroxide solution for deprotonation.[25,26] This Pani would be used to coat the nickel current collectors in next section.

### Coating the polyaniline films onto treated nickel current collectors

To reduce the contact resistance between the metal current collector and the conducting polymeric electrode material, another type of sample was also prepared. The nickel foils were first chemically treated to improve the bonding ability before being coated by Pani.

The prepared Pani base samples were dissolved in 10 mL of 1-methyl-2-pyrrolidinone (NMP; Acros Organics, Morris Plains, NJ) for 24 h to obtain Pani base solutions with different concentrations. The nickel foils were immersed in 1*M* $H_2SO_4$ solution for 5 min before washing with acetone. Afterward, the foils were immersed in an aqueous solution of monosodium salt of 1,2-dihydroxyanthraquinone-3-

**TABLE I**
**Electrode Systems Prepared for Electrochemical Supercapacitors**

| | |
|---|---|
| Polyaniline/carbon nanotubes composite based electrodes (Pani/CNT) | Pure polyaniline-based electrode |
| | Pani/CNT composite containing 10 wt % polyaniline |
| | Pani/CNT composite containing 20 wt % polyaniline |
| | Pani/CNT composite containing 40 wt % polyaniline |
| | Pani/CNT composite containing 60 wt % polyaniline |
| | Pani/CNT composite containing 80 wt % polyaniline |
| | Pure carbon nanotubes-based electrode |
| Polyaniline-coated current collectors (PCCC) | (PA6.7) Alizarin-treated electrodes deposited with polyaniline base solution, including 6.7 mg of polymer in 10 mL solvent |
| | (PA16.7) Alizarin-treated electrodes deposited with polyaniline base solution, including 16.7 mg of polymer in 10 mL solvent |
| | (PA25) Alizarin-treated electrodes deposited with polyaniline base solution, including 25 mg of polymer in 10 mL solvent |
| | (PA50) Alizarin-treated electrodes deposited with polyaniline base solution, including 50 mg of polymer in 10 mL solvent |
| | (PA100) Alizarin-treated electrodes deposited with polyaniline base solution, including 100 mg of polymer in 10 mL solvent |
| | (PA250) Alizarin-treated electrodes deposited with polyaniline base solution, including 250 mg of polymer in 10 mL solvent |
| | (NPA25) Untreated nickel electrodes deposited with polyaniline base solution, including 25 mg of polymer in 10 mL solvent |
| | (Ni) Nickel electrode as a reference |

sulphonic acid (alizarin; Acros Organics; 50 mg alizarin/100 mL distilled water) for another 5 min, then cleaned with distilled water, and left to dry at room temperature. Finally, the electrodes were prepared by directly depositing 10 μL Pani base solution onto the treated nickel foils and allowed to dry at room temperature for 3 days. As illustrated in Table I, PA6.7, PA16.7, PA25, PA50, PA100, and PA250 were the codes used to identify the electrode systems deposited with Pani base solutions containing 6.7, 16.7, 25, 50, 100, and 250 mg polymer in 10 mL NMP, respectively. For comparison, one electrode pair was prepared by depositing Pani base solution, containing 25 mg polymer in 10 mL NMP, on the untreated nickel foils. This electrode system was coded as NPA25.

### Characterization of both Pani/CNT composites and Pani-coated current collectors

The powders of CNTs and Pani/CNT composites containing 20, 40, and 60 wt % Pani, respectively, were analyzed by using a scanning electron microscope (SEM; Zeiss SUPRA 50 VP, Gotlingen, Germany) to investigate morphologies of Pani/CNT composites. Next, Fourier transform infrared (FTIR) spectra of pure multiwalled CNTs, pure Pani, and Pani/CNT were recorded with a Nicolet 6700 (Thermo Electron Corp., Waltham, MA) spectrometer, respectively. Samples were milled with potassium bromide into very fine powder and then pressed into a thin pellet suitable for the analysis. FTIR characterization was done in the frequency range from 4000 to 400 $cm^{-1}$ with a resolution of 2.0 $cm^{-1}$.

Furthermore, the electrochemical capacitive performances of Pani/CNT electrodes and Pani-coated current collectors (PCCC) were evaluated separately using a two-electrode cell system. The Pani/CNT electrodes were fabricated by mixing 80 wt % active material with 20 wt % PTFE as binder. They were then pasted onto untreated nickel current collectors (1 cm × 1 cm) by using a conductive silver paste and pressed under 10,000 pounds at 500°F for 5 min. In both cases, a separator, glass fiber filter paper, after immersing in 1*M* $NaNO_3$ electrolyte, was placed between the two electrodes to form the test cell of Pani/CNT electrodes and PCCC.

Finally, the cyclic voltammetry, galvanostatic charge/discharge tests, and electrochemical impedance analyses of all the supercapacitor samples were

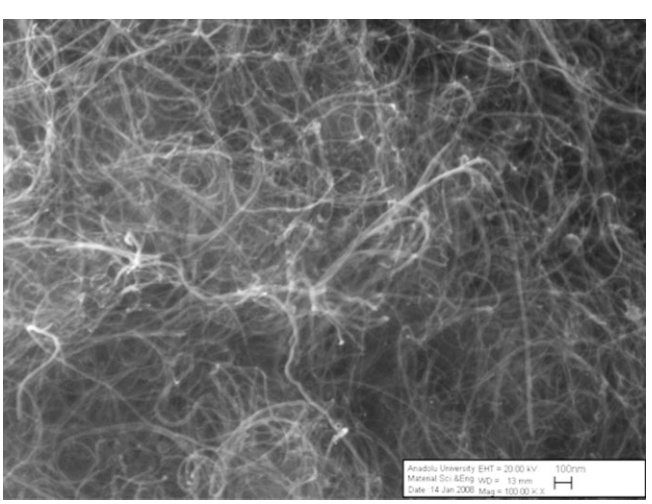

**Figure 1** SEM micrographs of pure carbon nanotubes (×100,000).

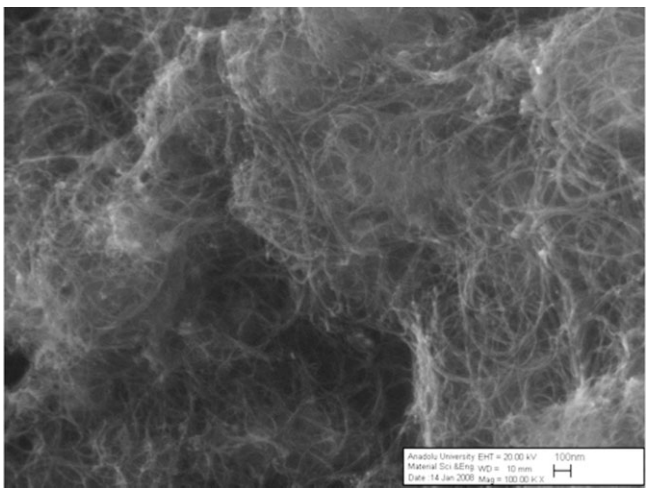

**Figure 2** SEM micrographs of Pani/CNT composite containing 20 wt % polyaniline (×100,000).

performed by using a Potentiostat/Galvanostat (Model 263A; EG&G Princeton Applied Research, Oakridge, TN). Cyclic voltammetry scans were recorded from 0 to 0.9 V at a scan rate of 50 mV/s. The charge/discharge tests were carried out at a discharge current of 1 mA on the Pani/CNT electrode systems, whereas at a discharge current of 0.1 mA on the PCCC system because the latter has less electrode materials. The impedance measurements were carried out by using EG&G 263A Potentiostat/Galvanostat with a frequency response detector in the frequency range from 50,000 to 0.05 Hz at an ac modulation of 10 mV.

## RESULTS AND DISCUSSION

### Polyaniline/CNT composite systems

Figure 1 shows the SEM image of pure CNTs, which are present in entangled form. It is difficult to disperse CNTs in the reaction medium of Pani synthesis so as to uniformly coat them. As shown in Figures 2–4, the micrographs do not illustrate a homogeneous coating of CNTs with Pani, indicating that the conducting polymer tends to grow both on itself and on CNT agglomerates. This may be one reason for relatively low capacitance values obtained by Pani/CNT systems because the Pani layer coated on nanotubes should be as thin as possible to protect the nanoporous three-dimensional morphology of CNTs so as to benefit from both the double-layer capacitance and the pseudocapacitance behavior of the composite constituents.[22–24]

FTIR is performed to identify and characterize the synthesized CNTs and Pani. Besides, it is also used to examine the coating quality between the polymer and CNTs and the possible interactions between the constituents in the Pani/CNT composite. Figure 5(a)

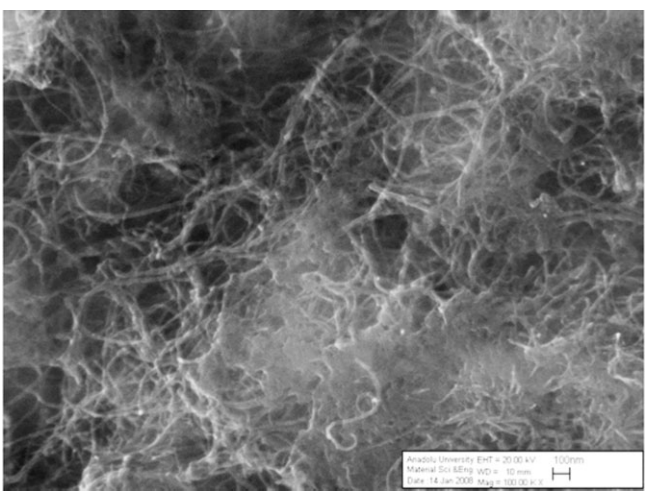

**Figure 3** SEM micrographs of Pani/CNT composite containing 40 wt % polyaniline (×100,000).



**Figure 4** SEM micrographs of Pani/CNT composite containing 60 wt % polyaniline (×100,000).

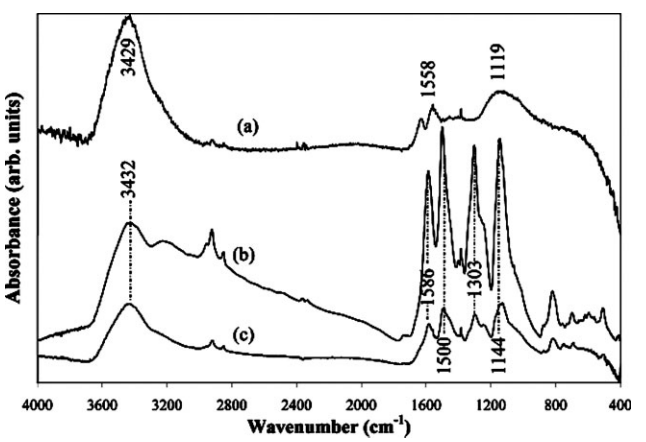


**Figure 5** Comparison of FTIR spectra of (a) pure carbon nanotubes, (b) pure polyaniline, and (c) polyaniline/carbon nanotubes (Pani/CNT) system containing 40 wt % polyaniline.

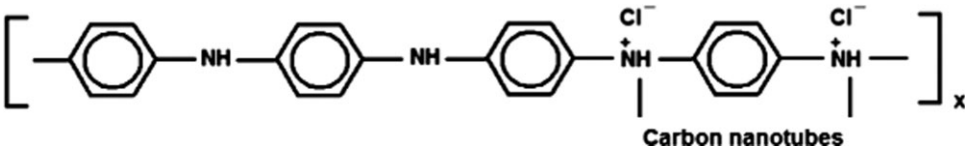


**Figure 6** Possible reaction between polyaniline and carbon nanotubes during the polymerization process.[27,42]

presents the FTIR spectrum of pure multiwalled CNTs. The peak at 3429 $cm^{-1}$ represents the presence of hydroxyl group (—OH) on the surface of CNTs, likely resulted either from oxidation during purification of nanotubes or from the ambient moisture bound to the CNTs.[28–31] Another band at 1633 $cm^{-1}$ is attributed to the C=O stretching of quinone groups on the surface of CNTs.[28,30,31] The peak at 1558 $cm^{-1}$ is corroborated to characteristic stretching vibrations of C=C.[32] In addition, the peak at 1384 $cm^{-1}$ is attributed to the bending vibration of the —OH group,[30] and a band at 1119 $cm^{-1}$ to the stretching vibration of C—O.[33]

Analysis of the FTIR spectrum for Pani [Fig. 5(b)] shows the following typical characteristics including the N—H peak at 3432 $cm^{-1}$ [19,34]; peak at 2923 $cm^{-1}$ attributed to the stretching vibration of C—H[19,35]; peaks at 1586 and 1500 $cm^{-1}$ for the characteristic C=C stretching of the quinoid and benzenoid rings, respectively[36]; peak at 1384 $cm^{-1}$ related to the C—N stretching mode; peak around 1303 $cm^{-1}$ corroborated to C—N stretching of tertiary aromatic amine in the quinine di-imine unit.[36,37] Another characteristic peak at 1144 $cm^{-1}$ is attributed to the vibration mode of $—NH^{+}=$ structure due to protonation,[34] the peak at 819 $cm^{-1}$ to the out-of-plane bending vibration of C—H,[38] and the peak at 698 $cm^{-1}$ due to vibration mode of the C—C band of the aromatic nuclei.[39]

It is observed in Figure 5(c) of the Pani/CNT composite that the peak at around 3432 $cm^{-1}$ becomes the most prominent,[19,34,40] a combined result of the 3429 $cm^{-1}$ peak of the CNTs and 3432 $cm^{-1}$ peak of Pani. The enhanced intensity of this N—H peak indicates an increased structural order due to better alignment of the coated polymer chains, a sign of an accomplished polymerization reaction in the presence of CNTs,[34] illustrating two new absorption bands, one at 2850 $cm^{-1}$ and the other at 750 $cm^{-1}$. The peak at 2850 $cm^{-1}$ is assigned to C—H stretching vibration of the chemisorbed hydrogen on CNTs.[28,41] The 750 $cm^{-1}$ peak is due to the deformation vibration of the quinoid ring caused by the interactions between Pani and CNTs during the *in situ* polymerization process as depicted in Figure 6.[27,42] It is notable that the peaks observed at 1384 and 818 $cm^{-1}$ for pure Pani remain in Figure 5(c) for the Pani/CNT system.[38,43] The peaks for Pani at 2923, 1586, 1500, 1303, 1144, and 698 $cm^{-1}$ shifted to 2920, 1584, 1495, 1297, 1129, 691 $cm^{-1}$, respectively, in Figure 5(c).[19,26,35,36,39,44–46] Most other peaks for the Pani stayed in Figure 5(c) but with more or less deviation due to the interaction with nanotubes.[46] In general, the spectrum of the Pani/CNT system resembles more to that of the pure Pani than to that of the pure CNT.

However, the FTIR spectra of the Pani/CNTs systems containing different amounts of Pani are very similar to each other (Fig. 7). The amplitudes of the peaks reduce continuously as the Pani composition decreases from 80 to 10%. In addition, the bands

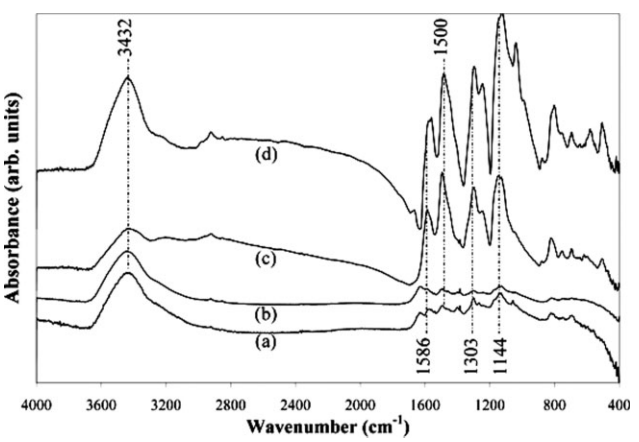


**Figure 7** Comparison of FTIR spectra of Pani/CNT systems containing (a) 10 wt % polyaniline, (b) 20 wt % polyaniline, (c) 60 wt % polyaniline, and (d) 80 wt % polyaniline.

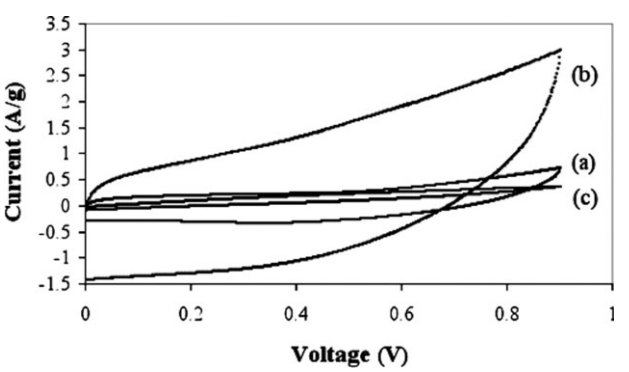


**Figure 8** Cyclic voltammetry curves of (a) pure carbon nanotubes, (b) Pani/CNT system containing 20 wt % polyaniline, and (c) pure polyaniline (scan rate: 50 mV/s).

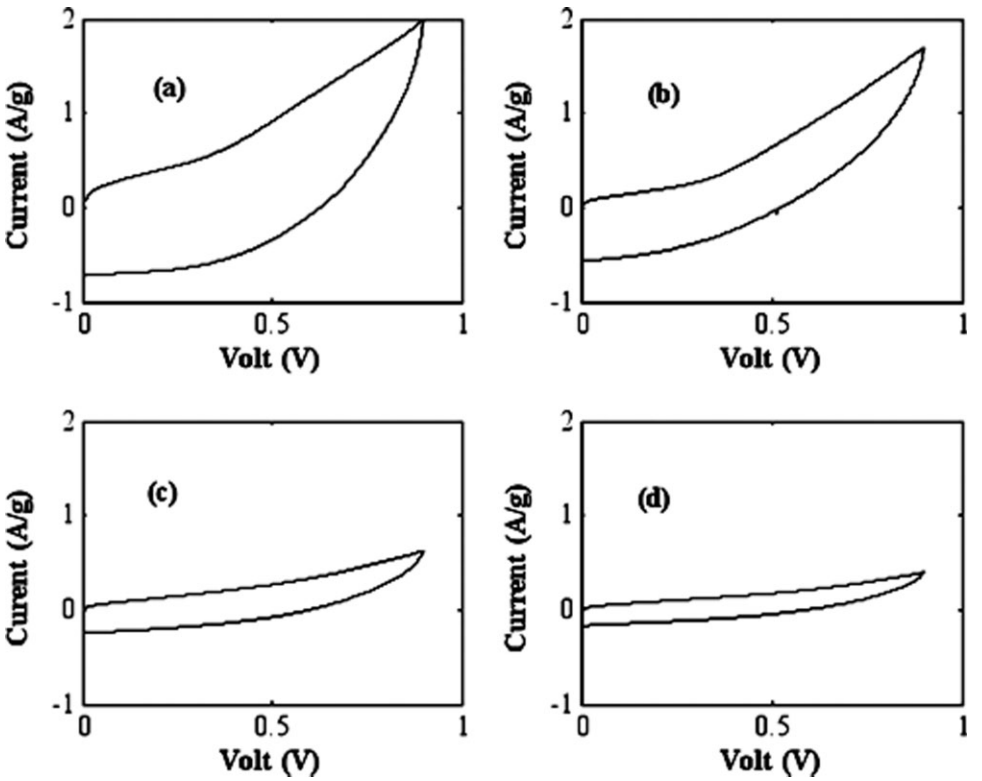


**Figure 9** Cyclic voltammetry curves of Pani/CNT composites containing (a) 10 wt % polyaniline, (b) 40 wt % polyaniline, (c) 60 wt % polyaniline, and (d) 80 wt % polyaniline (scan rate: 50 mV/s).

corresponding to N—H stretching, C=C stretching of the quinoid ring and the benzenoid ring, vibration mode of $-NH^{+}=$ structure due to protonation, and π-electron delocalization induced in the Pani by protonation caused the peak variation in positions among the Pani/CNT systems with different amounts of Pani.

The cyclic voltammetry measurements are performed on Pani electrode from 0 to 0.9 V, within which Pani is not exposed to degradation reaction.[47] An ideal double-layer capacitor has a cyclic voltammogram in rectangular shape: the energy storage process is directly electrostatic and the resulting current is independent of the potential. Upon reversal of the potential scan, the sign of the current is changed right away.[48] However, cyclic voltammetry curves of prepared electrochemical supercapacitors (Figs. 8 and 9) illustrate narrower loops far from the ideal rectangular shape. Zhou et al.[22] also reported of being unable to obtain symmetric and rectangular-like current-potential responses with Pani/CNTs system in the neutral electrolyte medium, $NaNO_3$. Three factors are considered responsible. First, it is due to the high internal contact resistances. The second factor is related to the pseudocapacitance effect that charged with faradaic reactions is kinetically slow, compared to the electrostatic charging, thus resulting a delay in response.[48] Additionally, there are rapid voltage changes at the start of both charge/discharge processes, known as the infrared drop, due to the resistance of the electrolyte between the electrodes, creating the specific internal resistance known as the series resistance.[3,21,49,50]

The potential–time response of a charge process is not a mirror image of its corresponding discharge counterpart in either pure nanotubes, pure Pani, or Pani/CNT composites as seen in Figures 10 and 11. Hence, these systems do not exhibit the ideally

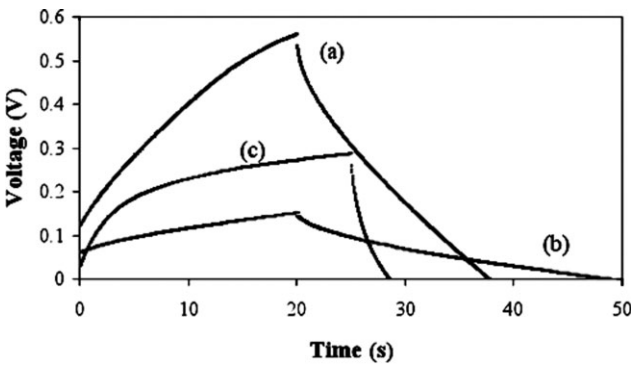


**Figure 10** Charge/discharge plots of (a) pure carbon nanotubes, (b) Pani/CNT system containing 20 wt % polyaniline, and (c) pure polyaniline (discharge current: 1 mA).

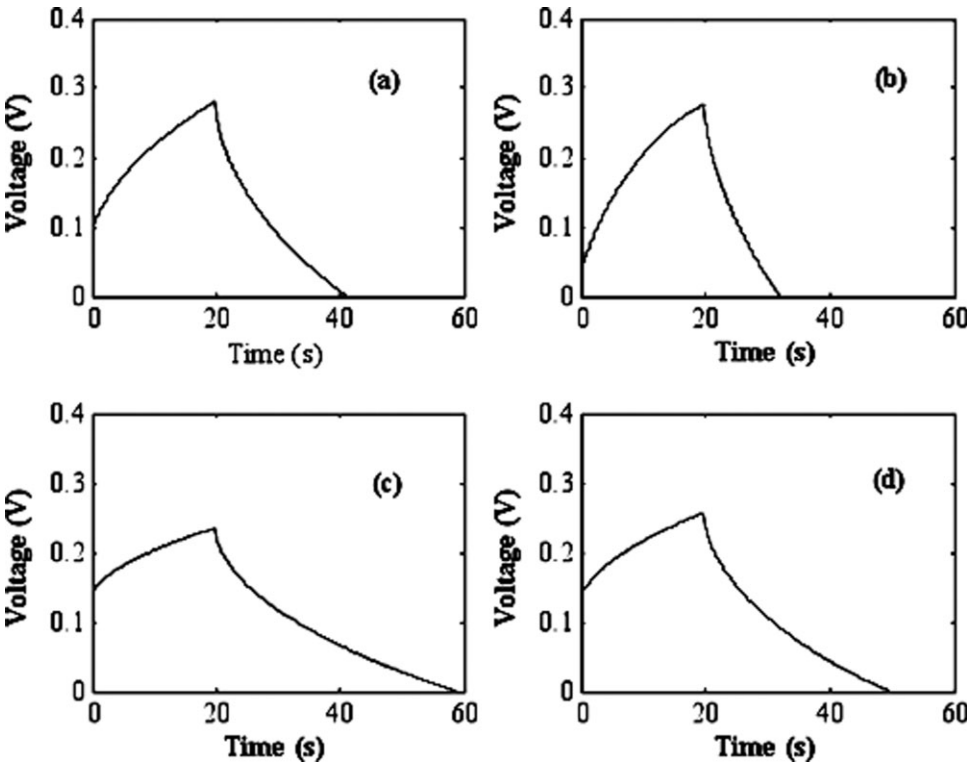


**Figure 11** Charge/discharge plots of Pani/CNT composites containing (a) 10 wt % polyaniline, (b) 40 wt % polyaniline, (c) 60 wt % polyaniline, and (d) 80 wt % polyaniline (discharge current: 1 mA).

capacitive behavior in 1*M* $NaNO_3$ electrolyte.[22] The specific capacitances $C_s$ for CNTs, Pani, and Pani/CNT composites were calculated from the galvanostatic charge/discharge plots by using the following relationships[15]:

$$C = \frac{I}{dV/dt} \tag{1}$$

$$C_s = \frac{C}{M} \tag{2}$$

where $I$ is the discharge current in amperes, $dV/dt$ is the slope in volt per second, and $M$ is the mass of the two active electrode materials in grams.[15] Pure CNTs result in low specific capacitance around 4 F/g, similar to the value obtained by Show and Imaizumi.[49] As displayed in Figure 12, electrochemical capacitance increases with Pani content until it reaches 20 wt % and then starts to decline. The highest specific capacitance of 20 F/g is obtained with the composite system containing 20 wt % Pani, likely the optimal pseudocapacitance contribution of Pani through oxidation–reduction reactions to the electric double-layer capacitance of CNTs.[51] More specifically, when compared with other systems, Pani at 20 wt % composition may have more porous surface structure, providing a

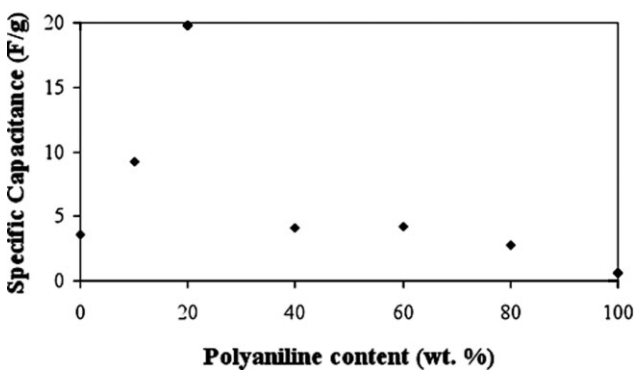


**Figure 12** Relationship of polyaniline content in Pani/CNT systems with the specific capacitance, calculated based on charge/discharge plots.

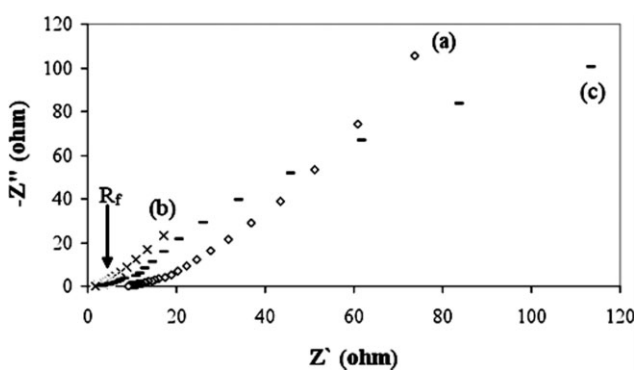


**Figure 13** Electrochemical impedance spectra of (a) pure carbon nanotubes, (b) Pani/CNT system containing 20 wt % polyaniline, and (c) pure polyaniline.

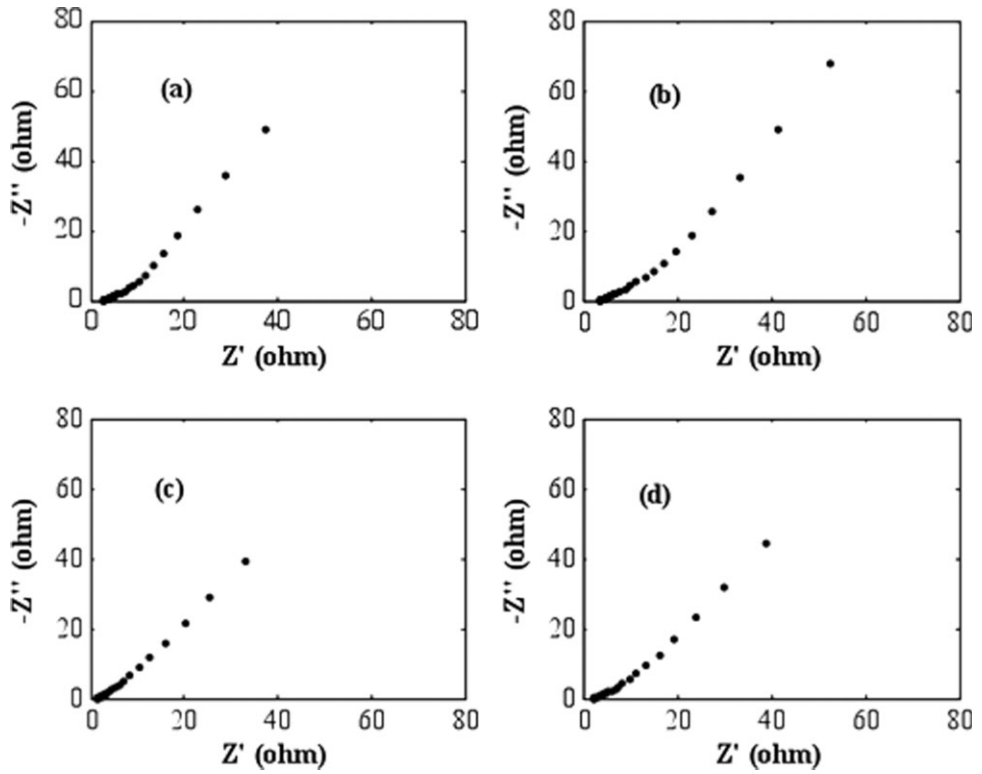


**Figure 14** Electrochemical impedance spectra of Pani/CNT composites containing (a) 10 wt % polyaniline, (b) 40 wt % polyaniline, (c) 60 wt % polyaniline, and (d) 80 wt % polyaniline.

larger specific surface area and also higher electronic and ionic conductivity. Larger specific surface area was reported to improve both the double-layer capacitance and the pseudocapacitance behavior of electrochemical capacitor at the same time.[15]

It is also observed before that the pseudocapacitance mechanism of electrochemical capacitor dominates with increasing conducting polymer content of Pani/CNTs systems.[51] However, in our case, the specific capacitance illustrates a reduction trend with a further increase in Pani content after 20 wt % composition. The only reason for this reduction may be that further increase of Pani content may cause reduction in specific surface area of Pani on CNTs. This trend may reveal that the double-layer capacitance behavior is more dominant than the pseudocapacitance behavior in the prepared capacitor.

The contact resistance between the active electrode material and the current collector is a critical factor in determining the performance of the electrochemical supercapacitors. Pressing of electrode material directly onto nickel foil likely results in high contact resistance, as indicated in Figures 13 and 14. Contact resistance between electroactive electrode material and nickel foil is considered to be part of the equivalent series resistance.[4]

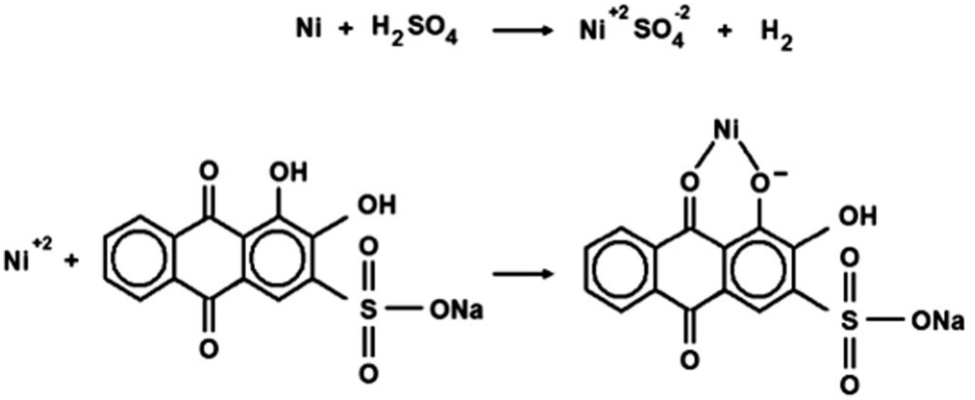


**Figure 15** Treatment of nickel foil with sulfuric acid and then with alizarin.[52,53]

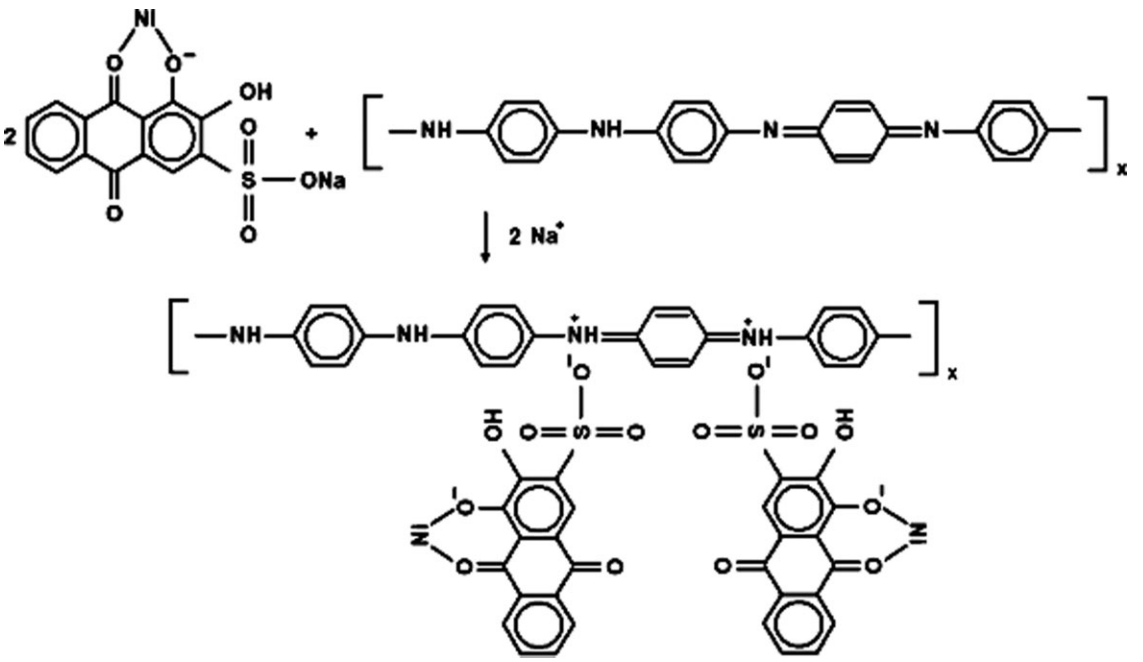


**Figure 16** Coating of treated nickel foil with polyaniline base using alizarin.[52,53]

The inner integrated area of cyclic voltammogram of Pani/CNTs-based capacitor (i.e., the power density) is higher than that of Pani and CNTs-based supercapacitors (Fig. 8). This may be due to the smaller internal resistance of Pani/CNT electrode.[50] The complex-plane impedance plot can be used to compare the electrical resistance of different electrode materials when the electrolyte resistance is held constant.[4] The results in Figures 8 and 13 confirm that the internal resistance of Pani/CNTs

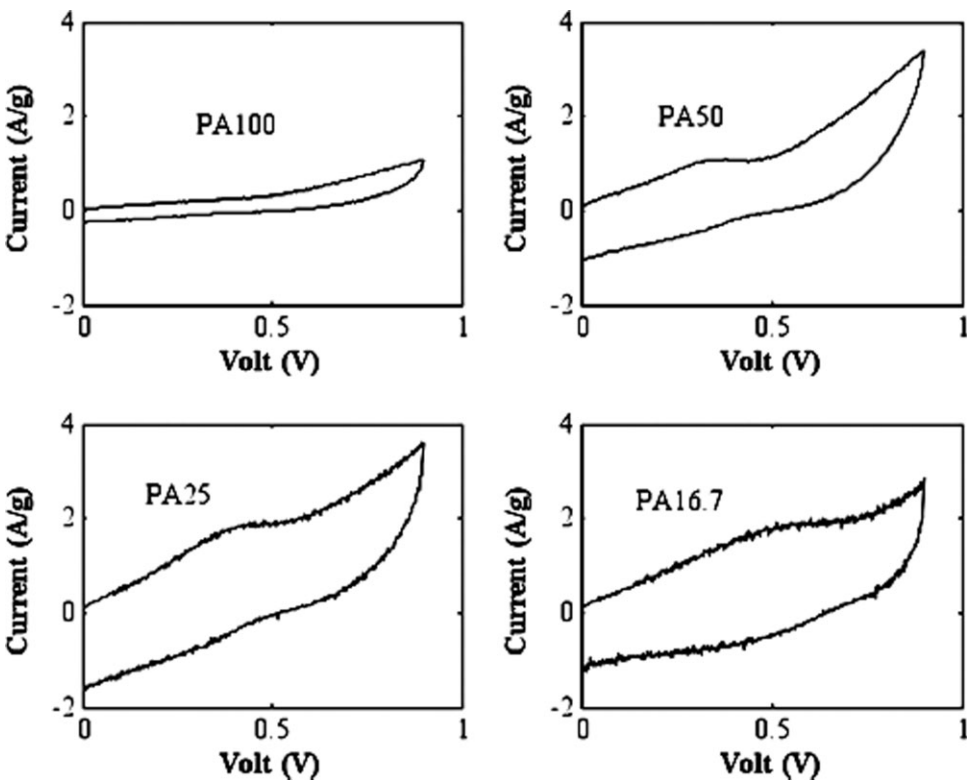


**Figure 17** Cyclic voltammetry plots of electrochemical supercapacitor with polyaniline-coated current collectors (PCCC) (scan rate: 50 mV/s).

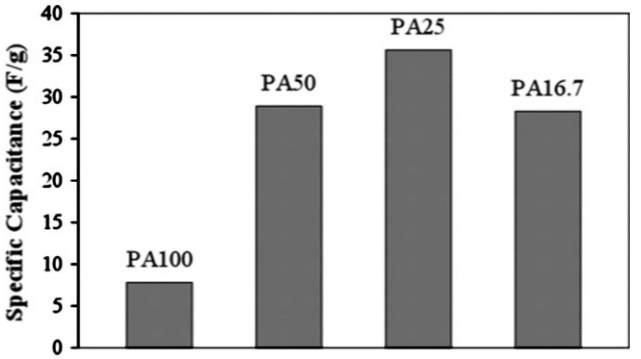


**Figure 18** Specific capacitance values of PCCC electrochemical supercapacitors.

electrode is lower than that of either the pure CNTs or the pure Pani electrodes (Figs. 8 and 13).

### Polyaniline film on alizarin-treated nickel foil

To improve the adhesion between the electrode constituents, alizarin treatment was applied to the current collectors because it has the ability to bind chemically both to the pretreated nickel surface and to the Pani film (Figs. 15 and 16).[52,53] Alizarin molecules bonded to nickel foils convert Pani base molecules to conducting form; that is, alizarin acts as a dopant when it bonds Pani molecules to nickel foil.

Capacitance results are expressed in F/g taking into account the weight of the whole electrode material, including Pani.[54] However, the accessibility of electrolyte ions into the pores inside the electrode is limited; that is, only certain parts of electrode material close to the interface between electrolyte and electrode can be used effectively during electrochemical capacitance measurements. To enhance the efficiency of the electrochemical supercapacitors, the thickness of the electrode material needs to be reduced, which leads to higher specific capacitances calculated from the integration of the area of the voltammogram.[54] Electrode systems PA100, PA50, PA25, and PA16.7 are lined up in an order that the thickness and the weight of the electrode material decrease from PA100 to PA16.7. The widest cyclic voltammetry curve and the highest specific capacitance (>35 F/g) are obtained with the electrode system PA25 (Figs. 17 and 18), likely the optimum Pani film thickness to provide higher specific capacitance. Specific capacitances cannot be calculated from the galvanostatic charge/discharge plots owing to fast potential-time response of discharge process (Fig. 19). Meanwhile, as shown in Figure 20, the electrical resistances $R_f$ for PA100, PA50, PA25, and PA16.7 electrode systems are at a similar level.[4]

PA250, NPA25, and PA6.7 electrode systems result in narrow cyclic voltammetry curves as pure nickel

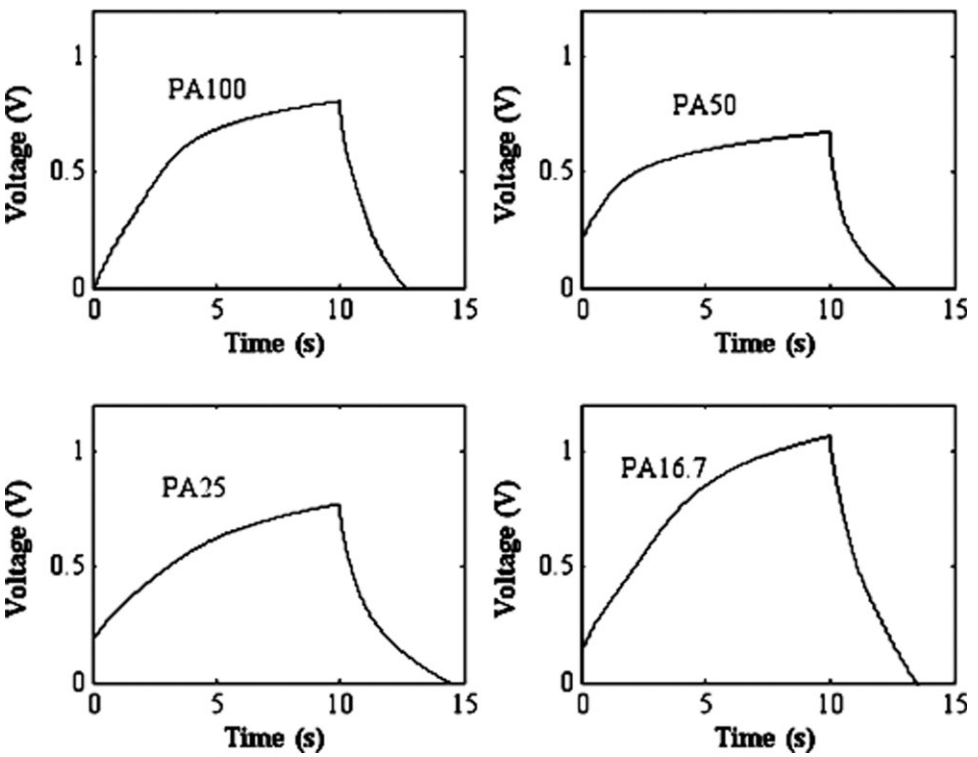


**Figure 19** Charge/discharge plots of PCCC electrochemical supercapacitors (discharge current: 0.1 mA).

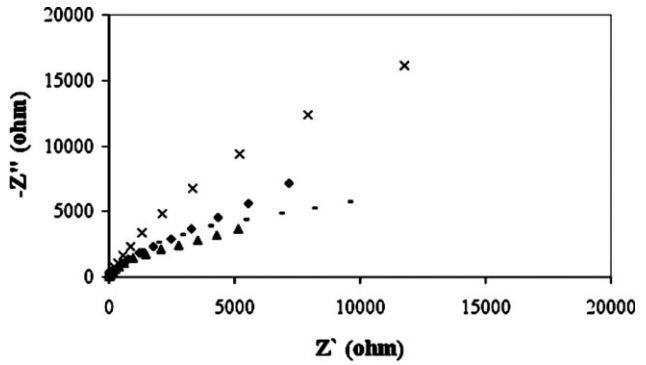


**Figure 20** Impedance spectra of PCCC electrochemical supercapacitors.

current collectors do (Fig. 21). First, the only difference between PA25 and NPA25 is that the PA25 system possesses alizarin-treated nickel foils, leading to the highest improvement and thus showing the effect of alizarin treatment of the foil. On the other hand, alizarin treatment does not seem to be effective at both PA250 and PA6.7 systems. Possible explanations may include that the alizarin may not be a very strong dopant when highly concentrated acid electrolyte is involved; also the doping effect of alizarin may be limited to a certain region close to the interface between nickel foil and Pani film. Besides, the accessibility of electrolyte ions into the pores inside the electrode is also restricted. Hence, the PA250 system, possessing the thickest electrode material of all, results in low capacitance. Conversely, the PA6.7 system does not contain adequate Pani.

Note that it is difficult to bond Pani in its conducting state, yet Pani will not be effective as electrode material in its insulating state. By using alizarin-treated nickel foil, both bonding and conducting capabilities of the Pani film are retained at the same time.

## CONCLUSIONS

Pani/CNT composites were prepared by an *in situ* polymerization of the conducting polymer in the presence of nanotube particles. Specific capacitances of the composite-based systems were higher than those of the electrode systems of either pure Pani or pure CNTs. However, capacitance values higher than 20 F/g could not be obtained with such composite-based electrochemical supercapacitors owing to poor electrode preparation technique, resulting in thick and rough electrode material on the current collector with high contact resistance. To enhance the performance of the electrochemical

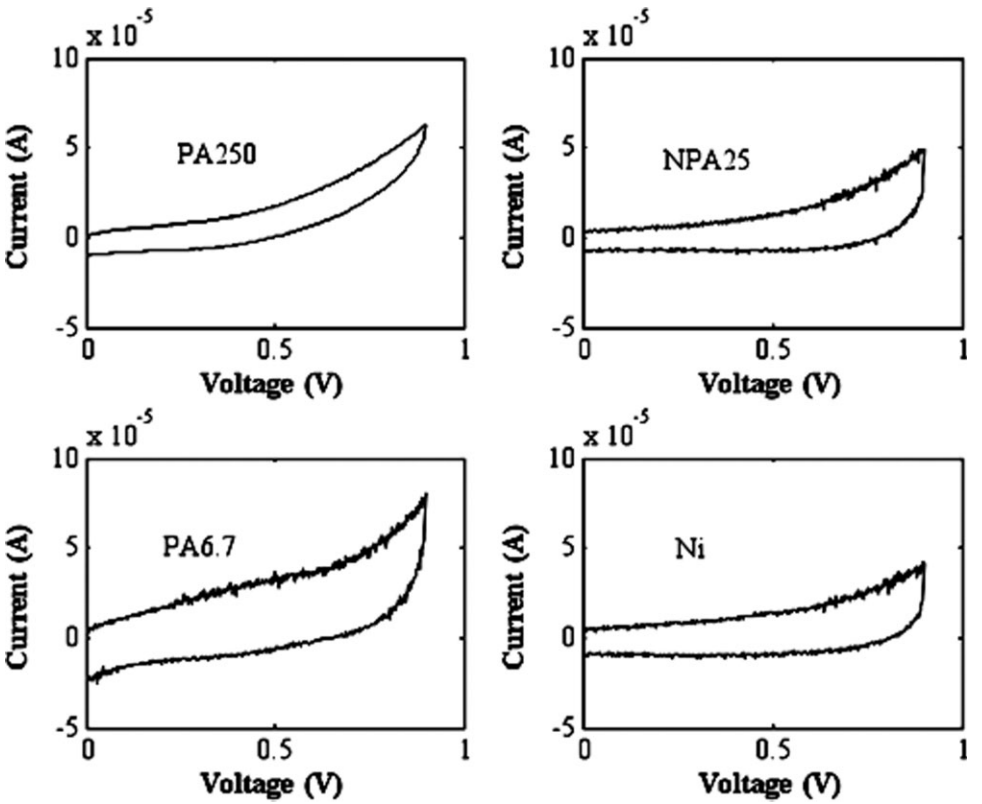


**Figure 21** Cyclic voltammetry plots of PCCC electrochemical supercapacitors and nickel current collector (Ni) as a reference (scan rate: 50 mV/s).

supercapacitors, the alizarin treatment was applied to nickel current collectors to improve the electrode material quality and reduce the contact resistance. The electrode system prepared directly by depositing Pani film onto alizarin-treated nickel foils achieved a higher specific capacitance (>35 F/g) than that of Pani/CNT-based systems.

## References


1. Arbizzani, C.; Mastragostino, M.; Scrosati, B. In Handbook of Organic Conductive Molecules and Polymers; Nalwa, H. S., Ed.; Wiley: Chichester, England, 1997.
2. Conway, B. E. Electrochemical Supercapacitors: Scientific Fundamentals and Technological Applications; Plenum Publications: New York, 1999.
3. Sarangapani, S.; Lessner, P.; Forchione, J.; Griffith, A.; Laconti, A. B. J Power Sources 1990, 29, 355.
4. An, K. H.; Kim, W. S.; Park, Y. S.; Choi, Y. C.; Lee, S. M.; Chung, D. C.; Bae, D. J.; Lim, S. C.; Lee, Y. H. Adv Mater 2001, 13, 497.
5. Frackowiak, E.; Metenier, K.; Bertagna, V.; Beguin, F. Appl Phys Lett 2000, 77, 2421.
6. Frackowiak, E.; Jurewicz, K.; Szostak, K.; Delpeux, S.; Beguin, F. Fuel Process Technol 2002, 77, 213.
7. Park, D.; Kim, Y. H.; Lee, J. K. Carbon 2003, 41, 1025.
8. Wen, S.; Mho, S. I.; Yeo, I. H. J Power Sources 2006, 163, 304.
9. Chatterjee, A. K.; Sharon, M.; Banerjee, R.; Neumann-Spallart, M. Electrochim Acta 2003, 48, 3439.
10. Yoon, B. J.; Jeong, S. H.; Lee, K. H.; Kim, H. S.; Park, C. G.; Han, J. H. Chem Phys Lett 2004, 388, 170.
11. Du, C.; Yeh, J.; Pan, N. Nanotechnology 2005, 16, 350.
12. Du, C.; Pan, N. J Power Sources 2006, 160, 1487.
13. Conway, B. E.; Birss, V.; Wojtowicz, J. J Power Sources 1997, 66, 1.
14. Ryu, K. S.; Kim, K. M.; Park, N. G.; Park, Y. J.; Chang, S. H. J Power Sources 2002, 103, 305.
15. Zhou, H.; Chen, H.; Luo, S.; Gewu, L.; Wei, W.; Kuang, Y. J Solid State Electrochem 2005, 9, 574.
16. Belanger, D.; Ren, X.; Davey, J.; Uribe, F.; Gottesfeld, S. J Electrochem Soc 2000, 147, 2923.
17. Zou, X.; Zhang, S.; Shi, M.; Kong, J. J Solid State Electrochem 2007, 11, 317.
18. Girija, T. C.; Sangaranarayanan, M. V. J Power Sources 2006, 156, 705.
19. Girija, T. C.; Sangaranarayanan, M. V. J Power Sources 2006, 159, 1519.
20. Gupta, V.; Miura, N. Mater Lett 2006, 60, 1466.
21. Fusalba, F.; Gouerec, P.; Villers, D.; Belanger, D. J Electrochem Soc 2001, 148, A1.
22. Zhou, Y. K.; He, B. L.; Zhou, W. J.; Huang, J.; Li, X. H.; Wu, B.; Li, H. L. Electrochim Acta 2001, 49, 257.
23. Frackowiak, E.; Khomenko, V.; Jurewicz, K.; Lota, K.; Beguin, F. J Power Sources 2006, 153, 413.
24. Gupta, V.; Miura, N. Electrochim Acta 2006, 52, 1721.
25. Stejskal, J.; Gilbert, R. G. Pure Appl Chemi 2002, 74, 857.
26. Konyushenko, E. N.; Stejskal, J.; Trchova, M.; Hradil, J.; Kovarova, J.; Prokes, J.; Cieslar, M.; Hwang, J. Y.; Chen, K. H.; Sapurina, I. Polymer 2006, 47, 5715.
27. Sun, Y.; Wilson, S. R.; Schuster, D. J Am Chem Soc 2001, 123, 5348.
28. Chen, G. X.; Kim, H. S.; Park, B. H.; Yoon, J. S. Polymer 2006, 47, 4760.
29. Choi, J. H.; Jegal, J.; Kim, W. N. J Membr Sci 2006, 284, 406.
30. Ma, P. C.; Kim, J. K.; Tang, B. Z. Carbon 2006, 44, 3232.
31. Deng, J.; Zhang, X.; Wang, K.; Zou, H.; Zhang, Q.; Fu, Q. J Membr Sci 2007, 288, 261.
32. Liang, Y.; Zhang, H.; Yi, B.; Zhang, Z.; Tan, Z. Carbon 2005, 43, 3144.
33. Choi, J. H.; Oh, S. B.; Chang, J.; Kim, I. I.; Ha, C. S.; Kim, B. G.; Han, J. H.; Joo, S. W.; Kim, G. H.; Paik, H. J. Polym Bull 2005, 55, 173.
34. Sengupta, P. P.; Adhikari, B. Mater Sci Eng A 2007, 459, 278.
35. Qiao, Y.; Li, C. M.; Bao, S. J.; Bao, Q. L. J Power Sources 2007, 170, 79.
36. Jing, S.; Xing, S.; Yu, L.; Wu, Y.; Zhao, C. Mater Lett 2007, 61, 2794.
37. Sengupta, P. P.; Barik, S.; Adhikari, B. Mater Manuf Process 2006, 21, 263.
38. Sazou, D.; Georgolios, C. J Electroanal Chem 1997, 429, 81.
39. Huang, J. E.; Li, X. H.; Xu, J. C.; Li, H. L. Carbon 2004, 41, 2731.
40. Amrithesh, M.; Aravind, S.; Jayalekshmi, S.; Jayasree, R. S. J Alloys Compd 2008, 458, 532.
41. Pal, A. K.; Roy, R. K.; Mandal, S. K.; Gupta, S.; Deb, B. Thin Solid Films 2005, 476, 288.
42. Lefrant, S.; Baibarac, M.; Baltog, I.; Mecellec, J. Y.; Godon, C.; Chauver, O. Diamond Relat Mater 2005, 14, 867.
43. Wei, D.; Kvarnstrom, C.; Lindfors, T.; Ivaska, A. Electrochem Commun 2006, 8, 1563.
44. Jurczyk, M. U.; Kumar, A.; Srinivasan, S.; Stefanakos, E. Int J Hydrogen Energy 2007, 32, 1010.
45. Gopalan, A. I.; Lee, K. P.; Santhosh, P.; Kim, K. S.; Nho, Y. C. Compos Sci Technol 2007, 67, 900.
46. Zengin, H.; Zhou, W.; Jin, J.; Czerw, R.; Smith, D. W.; Echegoyen, L.; Carroll, D. L.; Foulger, S. H.; Ballato, J. Adv Mater 2002, 14, 1480.
47. Barsukov, V. Z.; Khomenko, V. G.; Chivikov, S. V.; Barsukov, I. V.; Motronyuk, T. I. Electrochim Acta 2001, 46, 4083.
48. Frackowiak, E.; Beguin, F. Carbon 2001, 39, 937.
49. Show, Y.; Imaizumi, K. Diamond Relat Mater 2007, 16, 1154.
50. Wei, Y. Z.; Fang, B.; Iwasa, S.; Kumagai, M. J Power Sources 2005, 141, 386.
51. Tamai, H.; Hakoda, M.; Shiono, T.; Yasuda, H. J Mater Sci 2007, 42, 1293.
52. Ahmad, N.; MacDiarmid, A. G. Synth Met 1996, 78, 103.
53. Huerta-Vilca, D.; Moraes, E. S. R.; Jesus-Motheo, A. J Solid State Electrochem 2005, 9, 416.
54. Bleda-Martinez, M. J.; Morallon, E.; Cazorla-Amoros, D. Electrochim Acta 2007, 52, 4962.